Bioorganic & Medicinal Chemistry 18 (2010) 7804–7808

Contents lists available at ScienceDirect

Bioorganic & Medicinal Chemistry

journal homepage: www.elsevier.com/locate/bmc

Selective accumulation of a novel antimalarial rhodacyanine derivative, SSJ-127, in an organelle of *Plasmodium berghei*

Mayumi Ikegami-Kawai [a,*], Chika Arai [b], Yuko Ogawa [b], Ryohei Yanoshita [a], Masataka Ihara [b]

[a] *Faculty of Pharmaceutical Sciences, Hoshi University, 2-4-41 Ebara, Shinagawa, Tokyo 143-8501, Japan*
[b] *Institute of Medicinal Chemistry, Hoshi University, 2-4-41 Ebara, Shinagawa, Tokyo 143-8501, Japan*

ARTICLE INFO

Article history:
Received 29 July 2010
Revised 21 September 2010
Accepted 22 September 2010
Available online 26 September 2010

Keywords:
SSJ-127
Plasmodium berghei
Antimalarial rhodacyanine
Apicoplast
Mitochondrion

ABSTRACT

SSJ-127, a novel antimalarial rhodacyanine derivative, has shown potent antimalarial activity against chloroquine-resistant *Plasmodium* strains in vitro and subcutaneous administration of SSJ-127 results in a complete cure of a mouse malaria model. SSJ-127 was detected by fluorescence microscopy in the mouse malaria parasites *Plasmodium berghei* after exposure of infected red blood cells to the compound in vitro and in vivo. Selective accumulation of SSJ-127 in an organelle is observed in all blood stages of live malaria parasites. The organelle is clearly different from the mitochondrion and the nucleus in terms of morphology. The shape of the organelle changed during the asexual blood stages of the parasite. There was always a close association between the organelle and the mitochondrion. These results raised the possibility that SSJ-127 accumulates in an apicoplast of the malaria parasite and affects protozoan parasite-specific pathways.

1. Introduction

Malaria remains one of the world's most profound infectious diseases in terms of mortality and morbidity. In 2008, an estimated 243 million malaria cases occurred among half of the world's population at risk, causing nearly 863,000 deaths, mostly in children under 5 years. One hundred and eight countries were endemic for malaria in 2009.[1] There is still no effective vaccine for malaria. Furthermore, the spread of drug-resistant parasites and of insecticide-resistant mosquitoes causes additional problems.[2] The rapid development of strains resistant to existing antimalarial compounds has frustrated efforts to combat the disease. New chemotherapeutic targets are urgently required.

Malaria is caused by protozoan parasites of the genus *Plasmodium (P.)*, of which five species (*P. falciparum*, *P. vivax*, *P. malariae*, *P. ovale*, and *P. Knowlesi*) infect humans. *P. knowlesi* and other species such as, *P. yoelii*, *P. berghei*, *P. chabaudi*, and *P. gallinaceum*, infect a number of wild and domestic animals and are frequently used as models for the human parasites. *P. falciparum*, the most lethal species for human, is a unicellular eukaryote that undergoes a series of remarkable morphological transformations during the course of its multistage life cycle spanning two hosts (mosquito and human). In human red blood cells (RBCs), the malaria parasite undergoes a 48 h cycle of asexual replication and division. The early form following invasion, called the ring stage, is the phase of establishment in RBCs. The trophozoite stage is the most metabolically active biosynthetic phase, whereas the schizont stage represents the phase of nuclear division before release of merozoites from the erythrocyte. Many drugs target the functions of distinct organelles in each stage of *P. falciparum* development. Organelles of particular interest are the lysosomal food vacuole, the mitochondrion with a limited electron transport system, and the apicoplast (a plastid organelle thought to originate from a red algal symbiont).[3]

Previously, we have reported that the rhodacyanines, having a π-delocalized lipophilic cationic structure, exhibit strong antimalarial activities against *P. falciparum* in vitro.[4] Further investigation of a number of newly synthesized rhodacyanine derivatives led us to SSJ-127 (Fig. 1),[5] which when administered results in a complete cure of a mouse malaria model infected with *P. berghei*. SSJ-127 also exhibits strong antiprotozoal activities against chloroquine-resistant *P. falciparum*, *Trypanosoma brucei rhodesiense*, and *Leishmania donovani*, with low cytotoxicity against mammalian cells in vitro. In a recent report, Morisaki et al. demonstrated that

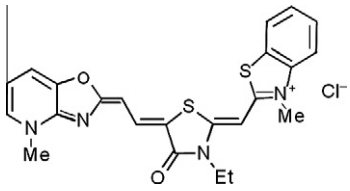

Figure 1. Structure of SSJ-127.

* Corresponding author. Tel.: +81 3 5498 5197; fax: +81 3 5498 5034.
E-mail address: m-kawai@hoshi.ac.jp (M. Ikegami-Kawai).

0968-0896/$ - see front matter © 2010 Elsevier Ltd. All rights reserved.
doi:10.1016/j.bmc.2010.09.054

some rhodacyanine derivatives accumulate in the mitochondrion of the parasite and are related to the inhibition of parasite growth.[6] However, their results were inadequate to ascertain whether the organelle was a mitochondrion. In this report, we demonstrate that SSJ-127 is rapidly accumulated in a specific organelle of a rodent malaria parasite, *P. berghei*, and examine the morphology of this organelle compared with that of the mitochondrion during the parasite's asexual life cycle in RBCs. These studies suggest on morphological grounds that the organelle is the apicoplast.

2. Results and discussion

2.1. Accumulation of SSJ-127 in *P. berghei* during asexual blood stages

The chemical structure of a novel rhodacyanine derivative, SSJ-127, is shown in Figure 1. SSJ-127 has a molar extinction coefficient of 3.88 ($\log \varepsilon$/L cm^{-1} M^{-1}) at 613 nm in water.[5] The fluorescence quantum yield of SSJ-127 is 0.0073 in methanol (Ex λ = 613 nm, Em λ = 635 nm) while the quantum yield of cresyl violet perchlorate is 0.54.[7] The fluorescence emission of SSJ-127, although not so strong, was expected to be sufficient for the detection of its localization in parasites.

To detect SSJ-127 in the parasite, we treated infected RBCs with SSJ-127 at 5×10^{-8} M, a concentration that approximates the IC_{50} value of SSJ-127 in in vitro experiments.[3] After incubation for 20 min at 37 °C, merozoites, released from matured schizont structures, and the parasite in RBCs were visualized using fluorescence microscopy. A comparison of fluorescence (SSJ-127), bright-field, and merged images of infected RBCs showed that SSJ-127 rapidly entered all parasites including free merozoites and intercellular forms, and accumulated in a small well defined focal area (Fig. 2), which we interpret as an organelle. Accumulation of SSJ-127 was observed in all blood stages of the parasite (Fig. 2, panels a–e). These organelles were round in shape at the merozoite and ring stages (Fig. 2a and b), and elongated during the trophozoite stage (Fig. 2c and d). In late trophozoites, the organelle was greatly expanded and had an extensive area of contact with the food vacuole, which showed crystalline particles of hemozoin (Fig. 2d, arrows). In parasites at the late schizont phase, multiple small rounded fluorescent organelles were visible (Fig. 2e). To examine the selectivity of SSJ-127 for the parasites, uninfected RBCs from normal mice were exposed to SSJ-127. At the concentration of SSJ-127 used, the fluorescence in the compartments was scarcely detectable. Infrequently, several small spots were observed in a reticulocyte of uninfected RBCs (data not shown).

In an in vivo experimental model, RBCs from infected mouse treated with SSJ-127 was examined. We have previously reported that the effect of SSJ-127 in vivo.[5] Three times administrations of 40 mg/kg/day of SSJ-127 provided 100% suppression and all treated mice have survived after 18 months (n = 3). Moreover, a pharmacokinetic study in male rats demonstrated excellent subcutaneous bioavailability of SSJ-127.[5] In this study, we examined to demonstrate the localization of SSJ-127 in RBCs of infected mouse. SSJ-127 (40 mg/kg body weight) was administered subcutaneously to infected mouse and blood was sequentially obtained from the tail vein.[5] Infected RBCs were directly observed in thin blood smears. Interestingly, the organelles, which shaped round, elongated, or branched, were shown in infected RBCs similarly to that in an in vitro study. This accumulation was sustained for at least 23 h (data not shown). After 23 h of administration, the parasitemia was decreased in SSJ-127 treated mouse from 13.0% to 10.8% and that of untreated mouse was markedly increased from 8.2% to 25.3%.

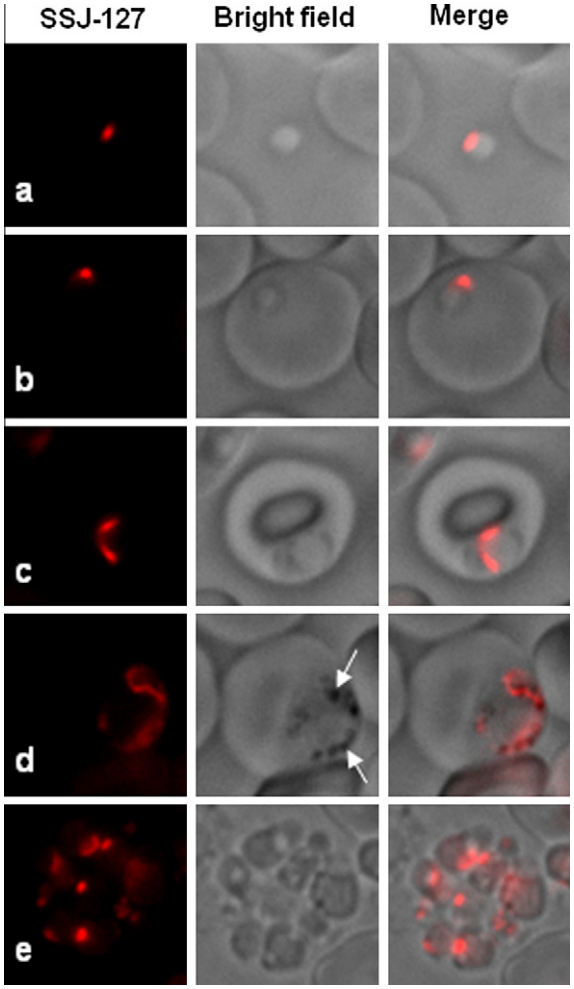

Figure 2. Accumulation of SSJ-127 in blood stages of *P. berghei*. Live infected RBCs were incubated with SSJ-127 (5×10^{-8} M) for 20 min at 37 °C. Fluorescent images were acquired using fluorescence microscopy (fluorescence filter cube: TX2, Leica Microsystems) as described in the Section 4. Fluorescent images of the SSJ-127-accumulating organelle (red), bright-field images, and merged images are shown. SSJ-127 was observed in a merozoite released from a matured schizont (a) and in RBCs at ring stage (b), early trophozoite stage (c), late trophozoite stage (d), and schizont stage (e). In panel d, the arrows denote crystals of hemozoin.

2.2. Effects of SSJ-127 on accumulation of Rhodamine 123 in mitochondria

To examine the mode of action of SSJ-127, we used Rhodamine 123, a membrane potential-dependent probe, to detect possible mitochondrial damage. Following exposure to carbonyl cyanide 3-chlorophenylhydrazone (CCCP), antimycin A, or SSJ-127 for 20 min at 37 °C, RBCs from infected mice were mixed with Rhodamine 123, as described in the Section 4. Figure 3 shows fluorescence images of mitochondria in infected RBCs. In control infected RBCs, Rhodamine 123 accumulated in the slender elongated mitochondria of parasites, as reported previously.[8] As shown in Figure 3, pre-treatment with CCCP, a protonophore, or antimycin A, a mitochondrial respiratory chain inhibitor, dissipated the membrane potential. The CCCP treatment completely abrogated the fluorescence signal in mitochondria, while antimycin A pre-treatment markedly reduced the signal. By contrast, SSJ-127 had no effect on the accumulation of Rhodamine 123 at a concentration of 5×10^{-8} M, which corresponds to the IC_{50} value in vitro. It is known that Rhodamine dyes such as Rhodamine 123 should be used carefully in studies on mitochondrial physiology because

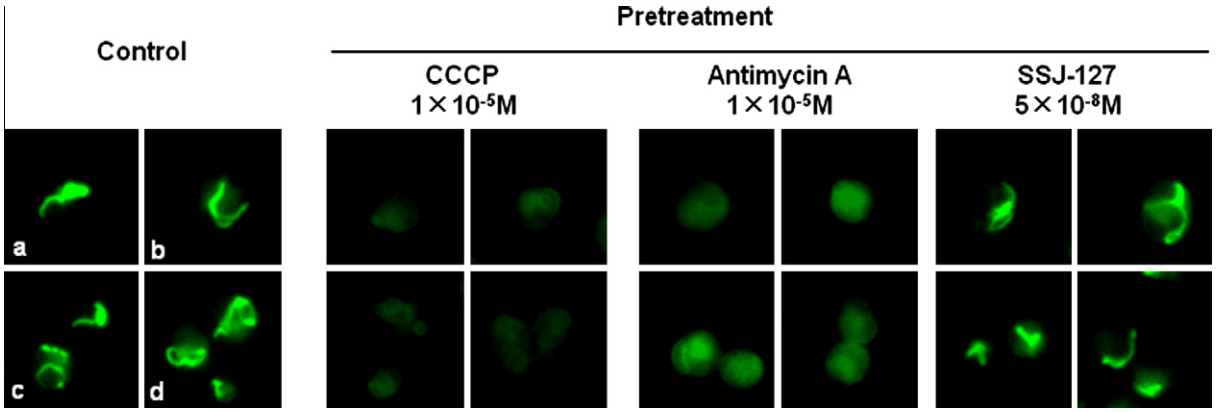

Figure 3. Effect of SSJ-127 on accumulation of R-123 in mitochondria in blood stages of *P. berghei*. Infected RBCs were incubated with CCCP (1×10^{-5} M), antimycin A (1×10^{-5} M), or SSJ-127 (5×10^{-8} M) for 20 min at 37 °C. Control infected RBCs received no additives. At the end of incubation, Rhodamine 123 (2.5×10^{-7} M) was added, followed by an additional incubation for 20 min. Fluorescence images were acquired using a Leica AF6000 fluorescence imaging system (fluorescence filter cube, L5). Each panel shows a single infected RBC, which included one (a, b) or a few trophozoites (c, d).

micromolar concentrations of such dyes have adverse effects on mitochondrial respiration.[9] However, after treatment of infected RBCs with Rhodamine 123 (2.5×10^{-7} M) for 20 min at 37 °C, SSJ-127 rapidly accumulated in the organelle in this study (data not shown). These findings suggest that accumulation of SSJ-127 in the organelle was independent of the mitochondrial membrane potential during an early event in the mechanism of action of SSJ-127.

2.3. Subcellular localization of SSJ-127 in blood stages of *P. berghei*

Since SSJ-127 has no effect on mitochondrial membrane potential, we examined the subcellular localization of the SSJ-127-accumulating organelle, the mitochondrion, and the nucleus in *P. berghei*. To visualize these organelles, infected RBCs were incubated simultaneously with SSJ-127, Rhodamine 123, and DAPI (4′,6-diamoidino-2-phenylindole). Figure 4 shows a fluorescence image of the SSJ-127-accumulating organelle, the mitochondrion, a merged image including the nucleus, and a bright-field all-merged image. Clearly, in terms of morphology, the SSJ-127-accumulating organelle differs from the mitochondrion labeled by Rhodamine 123 and the nucleus labeled by DAPI. In the ring and early trophozoite stages, the organelle was round or elongated, and its surface was in contact with the mitochondrion (Fig. 4a and b). However, as the organelle began to elongate in the late trophozoite stage, there were remarkably few apparent associations with the mitochondrion (Fig. 4c, two points of contact indicated by arrows). In the schizont stage, the majority of mitochondria were branched and the SSJ-127 accumulating organelle was also branched, and contact points between the two organelles increased in number (Fig. 4d). The organelle distributed into several new daughter cells, which were round in shape in late schizonts (Fig. 2e). The organelle and the mitochondrion were always closely associated during the asexual life cycle.

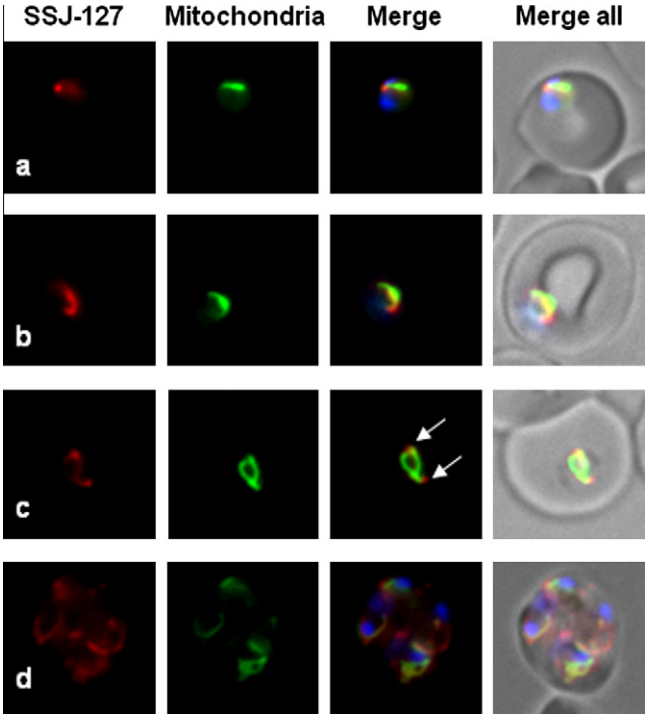

Figure 4. Subcellular localization of SSJ-127 in blood stages of *P. berghei*. Live infected RBCs were incubated with SSJ-127 (5×10^{-8} M), Rhodamine 123 (2.5×10^{-7} M), and DAPI (2.5×10^{-7} M) for 20 min. Fluorescent images of the SSJ-127-accumulating organelle (red), mitochondria (green), merged image including nucleus (blue), and a bright-field all-merged image are shown. Infected RBCs are shown at the ring stage (a), early trophozoite stage (b), late trophozoite stage (c), and schizont stage (d). In panel c, the arrows indicate two points of contact between the SSJ-12-accumulating organelle and the mitochondrion.

The morphology of the *P. falciparum* parasite has been well reported using electron microscopy and fused complexes formed by fluorescent reporter proteins containing organelle-targeting sequences.[10–14] *P. falciparum* contains numerous intracellular organelles that function during this asexual cycle. Certain organelles are believed to persist in all blood stages. For instance, all stages are assumed to exhibit endoplasmic reticulum (ER), an unusual unstacked Golgi compartment, the mitochondrion, and the apicoplast. Detailed associations of each organelle in *P. berghei* were not well understood until now. However, these organelles are expected to be similar to those of *P. falciparum*, since we know from electron micrographs that *P. berghei* possesses many organelles similar in structure to those of *P. falciparum*.[10,11] We attempted to compare the morphologies of organelles in *P. falciparum* with those in *P. berghei*.

The morphology of the ER and the Golgi compartment were reported using a transgenic parasite expressing green fluorescent protein (GFP) in *P. falciparum*.[12,13] These organelles and the SSJ-127-accumulating organelle in *P. berghei* differ in their morphologies in late stages of the parasite. The morphologies and relationship between mitochondria and apicoplast were revealed using a double-transgenic parasite targeting different specific markers in *P. falciparum*.[12] The mitochondrion is attached to the

apicoplast throughout the RBC cycle and divides up in the same way during schizogony. Three-dimensional reconstruction from serial electron microscopic sections allows detailed analysis of the *P. falciparum* structure.[10,13] These reports were supported by the observation of a physical binding between the two organelles.[15] Moreover, the organelle lies close to the food vacuole in trophozoites (Fig. 2d).[11] The morphology of the apicoplast is similar to the behavior of SSJ-127-accumulating organelle in *P. berghei* (Fig. 4). The organelle has the chief characteristics of the apicoplast as seen in *P. falciparum*, although with some minor differences of shape and size.[10,11,13]

Our results indicate that the target organelle of SSJ-127. The accumulation of SSJ-127 to the organelle was visible when infected RBCs were treated with SSJ-127 at 5×10^{-7} M that approximates the IC_{50} value in in vitro experiments. Similarly, fluorescent organelles were visible in parasites from SSJ-127 treated mouse leading to a cure. These results raised the possibility that SSJ-127 exhibits antimalarial activity as a result of its accumulation in the organelle. On the other hand, SSJ-127 is also toxic to *Trypanosoma brucei rhodesiense* and *Leishmania donovani* which lack apicoplast. Because the apicoplast contains a number of metabolic pathways that are present in bacteria and plants, the target pathway of SSJ-127 in malaria parasite is presumed to be different from that in these protozoa.

The recent discovery of apicoplasts in malarial parasites has opened new avenues in malaria research. It initiated the *P. falciparum* genome sequencing project, which revealed a number of biochemical pathways previously unknown to *Plasmodium*, namely, the cytosolic shikimate pathway, and apicoplast type II fatty acid, non-mevalonate isoprene, and heme biosyntheses.[16] Since these vital biosynthetic processes are absent in humans and fundamentally different from those found in humans, they represent excellent targets for pharmaceutical interventions. In this report, we demonstrate that SSJ-127 accumulates in a parasite-specific organelle, not in the mitochondrion. This study introduced the possibility that the organelle is an apicoplast of the malaria parasite. To confirm this possibility, co-localization of SSJ-127 with an apicoplast marker (e.g., parasites expressing a GFP-tagged apicoplast protein) should be demonstrated. Recently, the genetic transformation of *P. berghei* and the subsequent selection of transformed parasites expressing GFP were reported.[17,18] However, the method has many technical difficulties such as the drug-resistance selection in vitro and in vivo. Further investigations to confirm the status of the organelle are in progress with the goal of fully understanding the mechanisms of SSJ-127. We then expect that the novel antimalarial rhodacyanine derivative SSJ-127 may be a useful tool for live cell imaging of *Plasmodium* species.

3. Conclusion

We show that a novel antimalarial rhodacyanine derivative, SSJ-127, is detectable in malaria parasites in mouse RBCs using fluorescence imaging in vitro and in the experimental administered model. SSJ-127 selectively accumulated in an organelle in all blood stages of the parasite. The organelle was clearly different from the mitochondrion and the nucleus in terms of morphology. These observations raised the possibility that SSJ-127 accumulates in an apicoplast of the malaria parasite and affects protozoan parasite-specific pathways.

4. Experimental

4.1. Materials

Rhodamine 123 was purchased from Wako Pure Chemical (Osaka, Japan). DAPI nuclear stain was purchased from Molecular Probes, Inc. (Eugene, OR, USA). Antimycin A and CCCP were purchased from Sigma (St. Louis, MO, USA). All aqueous solutions were prepared using water filtered through a Milli-Q water system (Millipore, Bedford, MA, USA). All other chemicals were of reagent grade.

SSJ-127, Rhodamine 123, DAPI, CCCP, and antimycin A were dissolved in dimethylsulfoxide (DMSO) at 5 mM and stored at 4 °C. Subsequent dilutions were determined by the magnitude of dilution needed to reach the desired concentration in buffer A (116 mM NaCl, 5.4 mM KCl, 0.8 mM $MgSO_4$, 5.5 mM glucose, and 50 mM Hepes, pH 7.2).

4.2. Parasites

Strain NK 65 of *P. berghei* was maintained by syringe passage every week in female ICR mice (Japan Laboratory Animals, Tokyo, Japan), aged 4–8 weeks old. The infected mice were anaesthetized with ether and blood was collected by heart puncture in phosphate-buffered saline, pH 7.4, containing 10 unit/mL of heparin at approximately 30% parasitemia. Infected RBCs were observed in air dried thin blood smears stained with the Diff-Quik stain kit (Sysmex Corporation, Kobe, Japan). Control RBCs were obtained from uninfected mice.

In vivo studies were conducted to demonstrate the localization of SSJ-127 in infected mice. The mice were inoculated intravenously with 1×10^5 parasitized RBC (resuspended in 200 μL of normal saline solution) on day-0. On day-4, an infected mouse (27.4 g, 13.0% parasitemia) was subcutaneously administrated SSJ-127 (40 mg/kg body weight). Blood was sequentially obtained from the tail vein until 23 h after. As untreated control, blood of another infected mouse (28.0 g, 8.2% parasitemia) was similarly obtained without administration of SSJ-127. All experiments were performed in accordance with the Guiding Principles for Care and Use of Laboratory Animals at Hoshi University.

4.3. Fluorescence microscopy

Washed infected RBCs at a concentration of 1×10^7 cells/mL in buffer A were incubated in SSJ-127 (5×10^{-8} M) for 20 min at 37 °C. For measurement of the inhibitory effect of SSJ-127 on the accumulation of Rhodamine 123, washed RBCs were pre-incubated with CCCP (1×10^{-5} M), antimycin A (1×10^{-5} M), or SSJ-127 (5×10^{-8} M) for 20 min at 37 °C. At the end of the incubation period, Rhodamine 123 (2.5×10^{-7} M) was added, and the mixture was incubated for an additional 20 min. After incubation, treated RBCs were washed twice with buffer A by centrifugation at 4 °C and 700 *g* for 5 min. Nuclei and mitochondria were labeled using DAPI (2.5×10^{-7} M) and Rhodamine 123 (2.5×10^{-7} M), respectively, by incubation with RBCs for 20 min. After incubation, treated RBCs were washed twice with buffer A by centrifugation at 4 °C and 700 *g* for 5 min. Treated RBCs were resuspended in buffer A and visualized using Leica AF6000 fluorescence imaging system (Leica Microsystems, Wetzlar, Germany).

Acknowledgments

We thank Dr. Jian-Feng Ge, Hoshi University (present address: Soochow University) for technical advice. This study was supported by the Creation and Support Program for Start-ups from Universities, Adaptable and Seamless Technology Transfer Program through Target-driven R&D, Japan Science and Technology Agency (JST) and the Program for Promotion of Fundamental Studies in Health Sciences of the National Institute of Biomedical Innovation (NIBIO).

References and notes

1. World health organization. World malaria report 2009, 2009. Home page: http://www.who.int/malaria/world_malaria_report_2009/en/index.html (accessed Feb 2010).
2. Sibley, C. H.; Ringwald, P. *Malaria J.* **2006**, *5*, 48.
3. Rosenthal, P. J. *J. Exp. Biol.* **2003**, *206*, 3735.
4. Takasu, K.; Inoue, H.; Kim, H.; Suzuki, M.; Shishido, T.; Wataya, Y.; Ihara, M. *J. Med. Chem.* **2002**, *45*, 995.
5. Pudhom, K.; Ge, J.; Arai, C.; Yang, M.; Kaiser, M.; Wittlin, S.; Brun, R.; Itoh, I.; Ihara, M. *Heterocycles* **2009**, *77*, 207.
6. Morisaki, D.; Kim, H. S.; Inoue, H.; Terauch, H.; Kuge, S.; Naganuma, A.; Wataya, Y.; Tokuyama, H.; Ihara, M.; Takasu, K. *Chem. Sci.* **2010**. doi:10.1039/c0sc00125b.
7. Magde, D.; Brannon, J. H.; Cremers, T. L.; Olmsted, J., III *J. Phys. Chem.* **1979**, *83*, 696.
8. Divo, A. A.; Geary, T. G.; Jensen, J. B.; Ginsburg, H. *J. Protozool.* **1985**, *32*, 442.
9. Srivastava, I. K.; Vaidya, A. B. *Antimicrob. Agents Chemother.* **1999**, *43*, 1334.
10. Hopkins, J.; Fowler, R.; Krishna, S.; Wilson, I.; Mitchell, G.; Bannister, L. *Protist* **1999**, *150*, 283.
11. Ellis, D. S.; Li, Z. L.; Gu, M.; Peters, W.; Robinson, B. L.; Tovey, G.; Warhurst, D. C. *Ann. Trop. Med. Parasitol.* **1985**, *79*, 367.
12. van Dooren, G. G.; Marti, M.; Tonkin, C. J.; Stimmler, L. M.; Cowman, A. F.; McFadden, G. I. *Mol. Microbiol.* **2005**, *57*, 405.
13. Struck, N. S.; Dias, S. S.; Langer, C.; Marti, M.; Pearce, J. A.; Cowman, A. F.; Gilberger, T. W. *J. Cell Sci.* **2005**, *188*, 5603.
14. Bannister, L. H.; Hopkins, J. M.; Fowler, R. E.; Krishana, S.; Mitchell, G. H. *Parasitol. Today* **2000**, *16*, 427.
15. Kobayashi, T.; Sato, S.; Takamiya, S.; Komaki-Yasuda, K.; Yano, K.; Hirata, A.; Onitsuka, I.; Hata, M.; Mi-ichi, F.; Tanaka, T.; Hase, T.; Miyajima, A.; Kawazu, S.; Watanabe, Y.; Kita, K. *Mitochondrion* **2007**, *7*, 125.
16. Ralph, S. A.; van Dooren, G. G.; Waller, R. F.; Crawford, M. J.; Fraunholz, M. J.; Foth, M. J.; Tonkin, C. J.; Roos, D. S.; McFaddem, G. I. *Nat. Rev.* **2004**, *2*, 203.
17. Van Dijk, M. R.; Waters, A. P.; Janse, C. J. *Science* **1995**, *268*, 1358.
18. Janse, C. J.; Franke-Fayard, B.; Waters, A. P. *Nat. Protoc.* **2006**, *1*, 614.